







Research Article

Optimizing the Mechanical and Microstructure Characteristics of Stir Casting and Hot-Pressed AA 7075/ZnO/ZrO₂ Composites

P. Satishkumar ¹, **C. Saravana Murthi** ², **Rohinikumar Chebolu**,³
Yenda Srinivasa Rao ⁴, **Rey Y. Capangpangan** ⁵, **Arnold C. Alguno**,⁶
Vishnu Prasad Yadav,⁷ **M. Chitra** ⁸, and **Mahesh Gopal** ⁹

¹Anna University, Chennai, India

²Mechanical Engineering, United Institute of Technology, Coimbatore, Tamil Nadu, India

³Mechanical Engineering, Andhra University, Visakhapatnam, Andhra Pradesh, India

⁴Mechanical Engineering, Swamy Vivekananda Engineering College, Bobbili, Andhra Pradesh, India

⁵Department of Physical Science and Mathematics, College of Science and Environment, Mindanao State University, Naawan, Misamis Oriental, Philippines

⁶Department of Physics, Mindanao State University, Lligan Institute of Technology, Lligan City, Philippines

⁷Chemical Engineering, GGV, Bilaspur, India

⁸Electronic Communication Engineering, Kongu Engineering College, Tamil Nadu, India

⁹Mechanical Engineering, College of Engineering and Technology, Wollega University, Post Box No. 395, Nekemte, Ethiopia

Correspondence should be addressed to Mahesh Gopal; doctorgmahesh@gmail.com

Received 24 May 2022; Revised 4 July 2022; Accepted 8 July 2022; Published 8 August 2022

Academic Editor: Vijayananth Kavimani

Copyright © 2022 P. Satishkumar et al. This is an open access article distributed under the Creative Commons Attribution License, which permits unrestricted use, distribution, and reproduction in any medium, provided the original work is properly cited.

The composite was made using the stir cast manufacturing method. Many parameters, like stirring speed, stirring time, ZrO₂ reinforcement, and cast temperature, are evaluated in a Taguchi experimental design to see how they affected the composite properties. In terms of composite properties, ZrO₂% reinforcement and the stir speed have the most significant impact. There were 25.02% gains in ultimate tensile strength and hardness, as well as a decrease in composite wear loss, when the optimal stir casting parameters were used compared to the initial stir casting settings. To get insight into the process and the qualities of the composite, the hot-pressing parameters were studied. Pressure, followed by temperature, is the most critical factor in determining the properties of composites. When a hot-pressing setting was determined to reduce the wear loss by a significant 39.3%, it was deemed perfect by the superranking concept. Under ideal conditions, hot-pressing procedures reduced wear loss by 40.8% while boosting ultimate tensile strength and hardness by 19.83% and 9.6%, respectively. The resulting microstructures and worn surface morphologies from stir casting and hot pressing show vastly different properties.

1. Introduction

Al 7075-ZnO castings account for approximately 80% to 90% of the entire production of Al 7075 castings worldwide. There are a number of automotive and aerospace industries where Al 7075-ZnO castings have been used [1, 2]. These include the engine blocks, the cylinder heads of automobile engines, and transmission housings of automobile engines, as well as wheel rims, the powertrains, and suspension components of automobile engines [3–5]. Modern

businesses have developed composites (including reinforcements) that have improved toughness and plasticity, as well as the aforementioned qualities, as a result of technological breakthroughs [6]. Red mud, fly ash, borides, nitrides, oxide, and carbides are some of the reinforcing elements used in metal matrix composites (MMC) [7]. When it comes to porosity in composites, organic reinforcements may be more cost-effective. Because of the high temperatures, dynamic loads, and wear, composite material parts in these applications must have a greater level of hardness and wear

resistance. For piston, cylinder liner, and connecting rod applications, zirconium oxide (ZrO_2) reinforcement is good [8]. Sintering, casting, infiltration methods, spray forming, roll bonding, and equal channel angular pressing are some of the methods used to make these composites [9–11]. The most cost-effective processing procedures for MMCs are stir-casting and penetration, which account for around 67% of total volume output. Al 6061 alloy was strengthened and hardened by stirring in carbides (SiC and B₄C) before being cast. In Al 6063 stir-casting, SiC reinforcement of up to 12% increased hardness and strength [6]. Stir-cast hybrid composites with Silicon carbide and tungsten carbide reinforced Al6061 showed enhanced strength [3]. To some extent, the mechanical characteristics of composites are influenced by parameters related to stir-casting [12, 13]. Choosing the right variables to impact stir-casting parameters resulted in a better composite material's characteristics. When it comes to raising the quality of composites, it is assumed that conducting studies on all stir-casting factors one at a time is impractical [14, 15]. In addition to being time-consuming, tedious, wasteful, expensive, and energy-intensive, many methods are also inefficient. In addition, they produce regional solutions [16, 17]. For Al 7010 MMCs, Taguchi's statistical method limits practical testing to the lowest and most optimal stir-casting variables simultaneously [18]. The Taguchi method can be used to raise the hardness of MMC by adjusting the basal % of reinforcement, time, and size [19]. Silicon carbide reinforced AA6061 composites with the Taguchi technique's optimal parameter levels were shown to have improved wear resistance properties [20]. Stir-casting composites have varied densities because of the porosity created when reinforcing particles are added to the matrix material [20, 21]. Using porous materials in castings and composites can cause stress concentration and crack development [22]. When loaded, these components fail catastrophically due to their inferior tensile and fatigue strengths. MMC's with low porosity and a wide range of properties are still a problem to design using universal parametric criteria for novel matrix-reinforcement compositions. As a result, postprocessed composites require special attention to ensure that pores are sealed [23, 24]. Pores in composites can be minimized by some posttreatment methods such as extrusion, pressing, or rolling [25]. In 713LC superalloys subjected to hot pressing, this method increases fatigue life and decreases casting faults (porosity, microshrinkage, and inhomogeneity) [26, 27]. Cast Ti6Al4V exposed to various hot-pressing settings had their pore closure affected by pressure, temperature, and holding time. They discovered that the porosity of a hot-pressing material changes significantly depending on the parameters of the process [28–30]. It was found that using the Taguchi approach, pressure, temperature, and dwell time were all improved in Al 7075-5% TiC and that zirconium diboride composite density, grain size, and hardness were all improved using the Taguchi method [31]. The Taguchi approach was used to optimize the hot-pressing parameters and differences in silicon carbide percentage in ZrB₂ composites [32]. Differences in matrix-reinforcement compositions led Taguchi to calculate ideal hot pressing

settings, which were found to be different from previous studies [33]. Furthermore, there has been no effort to identify a single set of hot-pressing parameters that may be used for numerous outputs. Al-metal matrix composites have likely seen an improvement in mechanical and wear qualities due to the addition of reinforcement in the form of zirconium oxide [34]. It is the fundamental goal of the current research to develop Al 7075/ZnO reinforced with ZrO_2 (ZnO reinforced Al 7075). Stir-casting was used to create the composites [35]. Analysis and optimization of stir-casting parameters using the Taguchi method were utilized to increase wear resistance and hardness of the composites by increasing the stirring speed, stirring time, cast temperature and reinforcement weight percentage of ZrO_2 . The concept of super rank was used to optimize entire outputs [36]. Composites made with the concept of super ranking optimized stir-casting settings were hot pressed in order to close pores and increase their properties [34, 35]. Using the Taguchi approach, we were able to determine the best conditions for hot-pressing parameters in order to increase hardness and wear resistance [37]. Using the Pareto ANOVA technique, it is possible to identify the best possible conditions.

2. Materials and Methods

2.1. Materials. Matrix material for industrial applications using Al 7075/ZnO alloy: For use in load bearing applications, ZrO_2 has good hardness and wear resistance qualities as a reinforcing material. Stir-casting composites are created by adding ZrO_2 reinforcement to an Al 7075/ZnO alloy. At 50 μ m in diameter, the ZrO_2 particles were detected. According to an EDS analysis, the composite samples contain ZrO_2 , Al 7075, and ZnO.

2.2. Stir-Casting Method. Many sectors were interested in MMC's liquid state processing technique (stir casting) because of its durability, simplicity, and economy. For the fabrication of Al 7075/ZnO- ZrO_2 composites, melt stirring was facilitated by die casting. Mechanical stirring was used to disseminate ZrO_2 particles (4,8 and 12%) into a molten Al 7075/ZnO matrix metal. The precise selection of stirring speed, stirring time, reinforcement preheating, and melt temperature are all important for superior mechanical characteristics and homogenous ZrO_2 particle dispersion in the molten matrix. FENFE Metallurgical Laboratory in Bangalore provided the Al 7075/ZnO ingot material, which was then chopped into small pieces and deposited in a graphite container fitted with an electric furnace. First, the temperature of the specimen was raised to 780°C. Hexachloroethane (C_2Cl_6) tablets, pulverized into powder, are dipped into the molten metal below using a Zr-coated Cr-steel rod. The ZrO_2 powder reinforcements were heated to 525°C in an electric muffle furnace for 30 minutes to remove humidity, deposits, and scales from particles. Using a funnel, heat up particles added to melt and mechanically agitated at 525–625 rpm for 25–30 g/min. Finally, the heated mould was filled with the prepared melt and it was poured into the

mould to set (say 700 to 780°C). Using a split die, the casting was expelled from the die once it had solidified to the desired level of rigidity. With the use of a total of nine Taguchi tests (stirring speed, time, and temperature), we were able to find the best combination of ZrO₂ wt% (4,8 and 12%) and casting temperature. The results of each experiment are duplicated three times to ensure that they are accurate. An experimental stir-cast arrangement is depicted in Figure 1.

2.3. Hot-Pressing Method. Reduction of porosity and refinement of grains in the components are two of the primary reasons why the hot-pressing technique outperformed Stir Casting in terms of overall performance. As a result of this negative pressure differential, a vortex is formed that pulls in reinforcement and air bubbles, which results in pores or other defects in cast composite materials. In a hot-pressing procedure, the cast specimens are concurrently subjected to both pressure and warmth. In order to provide pressure, a 100-ton hydraulic press was used. An electric muffle furnace was used to heat the collected stir-cast samples. The desired experimentation temperature is maintained by the temperature control device (say 420–500°C). It took two hours to guarantee that the warmth was evenly distributed throughout the specimens by keeping them in a hot furnace. Fragmented die goes halves made of H13 Hot Work Steel are used to press specimens (45 HRC). Before using the die or punch, they must be heated to the proper temperature. There was a wide range of pressures and temperatures utilized in the hot-pressing process. The dwell duration was also changed (40, 80, and 120 MPa) (refer to Table 1). Pressure and heat were removed from the process after the proper dwell time had been established. The specimens were reexamined once they had cooled down.

2.4. Vickers Hardness Assessment. According to the ASTM E384 standard, Vickers hardness equipment was used to measure microhardness in composites of stir-cast and hot-pressed. Following milling and polishing, the specimens were ready for the hardness test. Tests for hardness were carried out in stir casting on the side opposite to the pressing and pouring directions. The composite specimens were subjected to a 1 kgf load for 10 seconds using a rectangular pyramid diamond indenter with a 136° angle. During the Vickers hardness test, each sample received an average of eight indentations.

2.5. Wear Test. The wear test was carried out using a computerized pin-on-disc (TR-20LE, Ducom) system. An ASTM-G99 standard operating method was used to note wear rate values, which were recorded. To ensure accurate results, the specimens were first polished to a surface roughness of 0.25 μm. Examples of pin materials utilized a range of stir-cast and hot-press processes. When the 8-inch-thick EN-24 steel disc is rubbed against the pin's substance, the hardness of the EN-24 steel (62 HRC) is maintained. Sliding at a speed of 2.5 meters per second and a distance of 1000 meters are utilized to record the wear rate data.

Welding tests are conducted in a temperature-controlled setting. For each of the hot-pressing and stir-casting settings, three wear rate results are averaged.

2.6. Tensile Strength. ASTM E8 standards were used to create and evaluate cast and hot-pressed samples. The tensile strength measurements were recorded using a universal testing machine. Tensile tests on every specimen were performed at a strain rate of 0.5 mm/s, as can be seen. The mean of tensile strength readings for each stir-casting and hot-pressing condition is recorded for each specimen.

2.7. Metallographic Examination. The metallic material's microstructure and production method have an effect on the material's physical, mechanical, and wear behavior. When 316 stainless steel pieces were subjected to a different production route, they displayed differential attributes and a varied microstructure. There is a substantial correlation between the change in microstructure and the change in properties. There have been similar findings reported in the literature. As a result, samples produced by stir-cast and hot-press are subjected to microstructural studies. The samples are first polished to a glass finish in order to be studied using optical and scanning electron microscopes. Composites' worn surface structure is examined using SEM.

2.8. Taguchi Method. Any manufacturing process can benefit from determining a set of optimal circumstances that enhances its product's performance. A trial and error or one factor at a time strategy results in this. There is a loss of time and money in addition to undesirable results [38]. The Taguchi approach has proven to be successful because of its solid experimental design and ability to address real-world problems with a minimum number of trials, even when there are several elements influencing the process's performance. The wear rate, UTS, and hardness of the stir-cast made Al 7075/ZnO-ZrO₂ composites are examined in Taguchi L9 tests to see how various parameters affect these composites (stirring speed, stirring time, temperature, and ZrO₂ reinforcements). Stir casting components and their relative values could only be identified after a thorough literature review [39]. Taguchi L9 trials were used to measure hardness, ultimate tensile strength, and wear rate as a function of hot-pressing factors (such as dwell time, pressure, and temperature). The conditions for hot pressing were established by a pilot experiment and subsequent study [40]. Table 1 shows the stir-cast or hot-press operations, experimentation, and optimization parameters and its levels.

2.9. Super Ranking Concept. Product/process performance can be improved using a Taguchi approach, although this method can only analyze and optimize certain reactions. It is possible to solve engineering problems using MCDM (multi-criteria decision making) approaches when many factors influence the responses that are in conflict with one another. There are a number of weighting methods that can be used for allocating individual responses, including

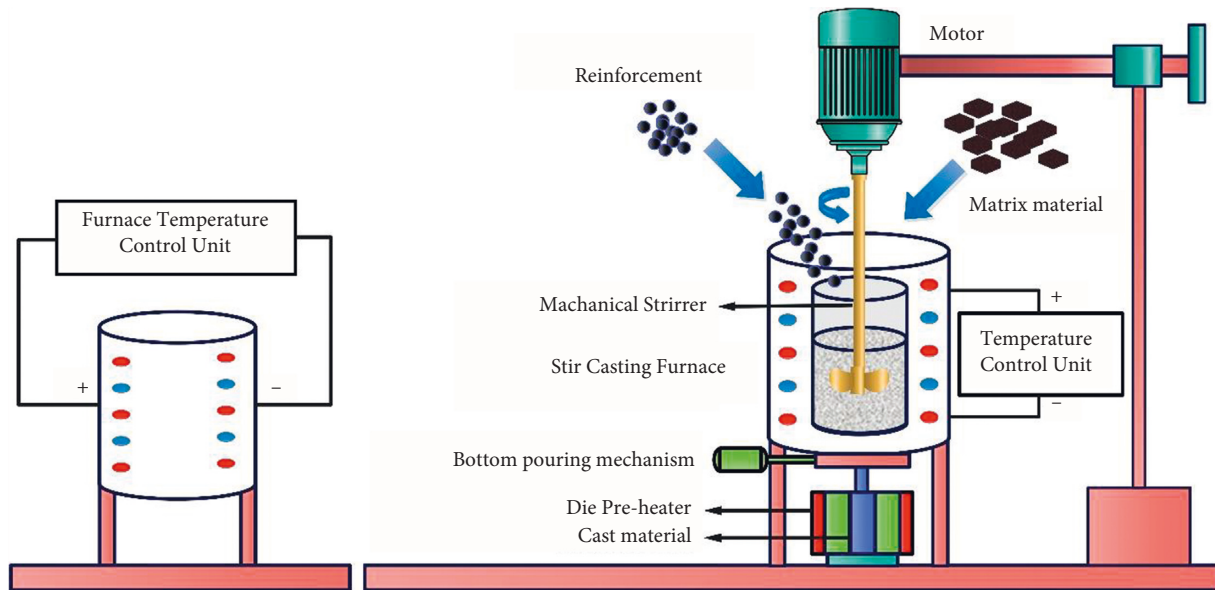


FIGURE 1: Schematic view of the stir-casting arrangement.

TABLE 1: Stir-cast progression and hot-press progression parameters.

Stir-cast progression		Hot-press progression	
Input parameters	Levels (1,2,3)	Input parameters	Levels (1,2,3)
A: Stirring speed, rev/min	525, 575, 625	E: Temperature, C	420, 460, 500
B: Stirring time, min	5, 10, 15	F: Pressure, MPa	40, 80, 120
C: Casting temperature, C	700, 740, 780	G: Dwelling time, min	15, 30, 45
D: ZrO ₂ reinforcement, %	4, 8, 12	-	-

CRITIC, PCA, and Entropy, Fuzzy and AHP. A skilled mathematician is needed to perform critical computational steps when analyzing contradictory optimization parameters when using weight methods. In order to quickly discover the best solutions, those in the sector require forecasting tools that utilize simple mathematical principles. SRC can be used to solve multi-objective optimization problems without the usage of weighting methods or costly computing procedures.

3. Results and Discussion

Microfluidic chip testing was conducted using a variety of stir-cast and hot-press settings on the Taguchi L9 microfluidic chip. Pareto analysis is used to discover optimal values for each parameter in the case of contradicting outputs. SRC is used to find a single set of optimal variables for all outputs in a model. Microstructure tests were carried out to support this. Using Taguchi and SRC's ideal circumstances as a baseline, independent experiments verify their conclusions.

3.1. Stir-Casting Process. To create the Al 7075/ZnO-ZrO₂ composites, stir casting was used. Taguchi L9 experiment method was used to examine the effects of stirring speed, stirring time, cast temperature, and ZrO₂ reinforcements (4,8,12%) on wear loss, hardness, and Ultimate tensile strength. For each trial, average values of 24 hardness

indents, three wear losses, and Ultimate tensile strength are shown in Table 2 based on a total of 36 indents. Using the actual output data, the S/N ratio was calculated. Quality parameters for hardness and UTS were employed with larger-the-better values, whereas wear loss was used with smaller values. Table 2 shows the S/N ratio statistics for the stir-casting process's output quality attributes.

In order to build the Pareto ANOVA, we used the S/N ratio data (Table 2). An analysis of variance using the Pareto principle helps researchers to find the elements that contribute and the best values for hardness and wear loss, as well as UTS.

3.1.1. Influence of Factors on Hardness. Using Signal to Noise ratio, Figure 2 depicts the hardness behavior for each factor and level. The results showed that adding ZrO₂ to the Al 7075/ZnO matrix at a higher percentage (after 12%) resulted in a significant decrease in hardness values. Possible explanations include an increase in trapped air within a ZrO₂ particle cluster when the ZrO₂ reinforcement percentage is increased, as well as the fact that ZrO₂ particles that have agglomerated during melting do not break apart. Some reinforced elements might aggregate on the melted surfaces to specific characteristics of MMCs. The shear action of rotating blade induced by a prolonged period of maximum stirring speed resulted in the deagglomeration of reinforcement particles in the melt mixture, resulting in a

TABLE 2: Experimental Input and output settings of stir-casting progression.

Trial. No	Input				Output			S/N ratio, dB		
	Stirring speed rpm	Stirring time Min	Casting temperature °C	ZrO ₂ reinforcement %	Hardness HV	Ultimate tensile strength MPa	WL Mg	Hardness	UTS	WL
L1	525	5	700	4	63.8	162.7	13.8	36.10	44.23	-22.80
L2	525	10	740	8	64.4	176.2	12.9	36.18	44.92	-22.22
L3	525	15	780	12	61.8	141.2	15.1	35.82	43.01	-23.58
L4	575	5	740	8	63.6	153.4	14.7	36.07	43.72	-23.35
L5	575	10	780	12	66.5	174.6	13.2	36.46	44.84	-22.41
L6	575	15	720	4	66.8	180.1	10.1	36.50	45.11	-20.09
L7	625	5	780	12	64.9	178.3	12.2	36.24	45.02	-21.73
L8	625	10	740	8	64.3	169.9	13.3	36.16	44.60	-22.48
L9	625	15	720	4	67.0	198.1	8.8	36.52	45.94	-18.89

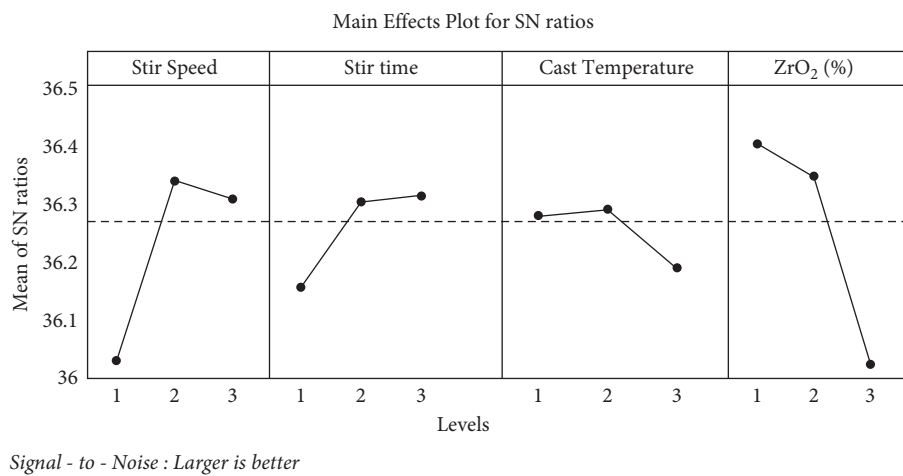


FIGURE 2: Main effect plot for hardness.

homogenous particle distribution in composites. Improved hardness values were achieved by increasing speed and stirring duration.

Observe that hardness ratings do not improve significantly once the stirring speed crosses the intermediate value. A possible explanation for the enhanced hardness values observed with a higher casting temperature is improved wettability and a more uniform mixing process. There was a strong correlation between ZrO₂ reinforcement and the effects of stirring rates, durations of stirs, and pouring temperatures (refer to Table 3). To maximize the hardness value, Pareto ANOVA indicated that A2B3C2D1 (i.e., 575 rpm, 15 min stir duration, 740°C cast temperature and ZrO₂: 4% ZrO₂) was found to be the best stir-casting conditions (refer Table 3). Owing to the multifactor structure of the studies (i.e., levels factors = 34 : 81 experimental set), the indicated ideal levels differ from those of L9 experiments.

3.1.2. Impact on Parameters on Wear Loss. Figure 3 illustrates the most important aspects that influence wear loss, as shown in the figure. After a 10% increase in ZrO₂ reinforcement to Al 7075/ZnO, wear loss increased. With an increase in the amount of ZrO₂ reinforcement, large particle clusters form that reduce matrix wetting and cause the

reinforcement to pull away from the matrix under loading conditions, leading to the formation of large gaps or pores in the composites. When the stir speed and time are increased, the wear loss lowers, allowing for a more uniform dispersion of reinforcement particles and an improved interparticle distribution. Particle agglomeration, on the other hand, can occur at modest stirring speeds and times. Increased wear loss is caused by cast temperatures which are either very less or very high. Over low pouring temperatures cause particle aggregation and premature solidification. Due to the long time it takes for the material to solidify at a high temperature, an undesirable microstructure can result. ZrO₂ reinforcement had the greatest impact on wear loss, followed by stirring time, stirring speed as well as pouring temperature. It was observed that A3B3C2D2 (i.e., 625 rpm, 15 minutes of stirring time, cast temperature of 740°C, and ZrO₂: 8% wt.) were the optimum parameter levels for decreasing wear loss in composites. In the Taguchi L9 trials, the optimal settings for minimising wear loss are not one of them.

3.1.3. Impact of Parameters on UTS. For the Al 7075/ZnO/ZrO₂ composites, the most important stir-casting factors were shown in Figure 4. From 4% to 12% ZrO₂ reinforcement, the ultimate tensile strength of the material did not

TABLE 3: Stir casting methodology for Pareto ANOVA results.

Output	Parameters	Levels	Stirring speed	Stirring time	Casting temperature	ZrO ₂ %	Total
Hardness (HV)	Mean	1	36.03	36.14	36.25	36.36	108.68
	Factor	2	36.34	36.27	36.26	36.31	—
	Levels	3	36.31	36.28	36.17	36.02	—
	Mean square deviation (MSD)		0.15	0.05	0.01	0.21	0.17
	% contribution		41.3	7.8	3.05	45.85	100
	Optimal levels			A2B3C2D1 (not at L9 experiments)			
Wear loss	Mean	1	-22.86	-22.62	-21.79	-21.37	-65.84
	Factor	2	-21.95	-22.37	-21.48	-21.34	—
	Levels	3	-21.03	-20.85	-22.57	-23.13	—
	MSD		5.05	5.48	1.92	6.32	18.77
	% contribution		27.93	28.4	11.12	32.78	100
	Optimum levels			A3B3C2D2 (not at L9 experiments)			
Ultimate tensile strength (MPa)	Mean	1	44.05	44.32	44.65	45.00	133.8
	Factor	2	44.56	44.79	44.86	45.02	—
	Levels	3	45.19	44.69	44.69	43.78	—
	MSD		1.96	0.34	0.47	3.06	5.84
	% contribution		34.29	5.15	7.34	53.22	100
	Optimum levels			A3B2C2D2 (not at L9 experiments)			

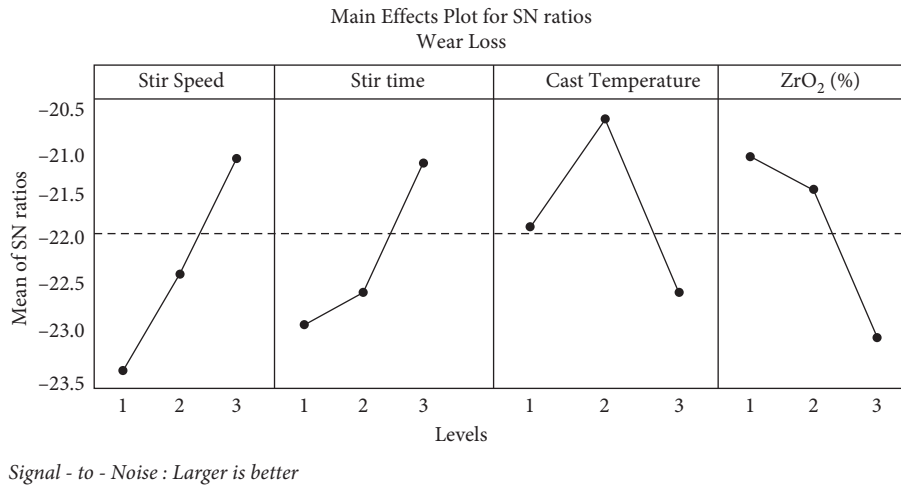


FIGURE 3: Main effect plot for wear loss.

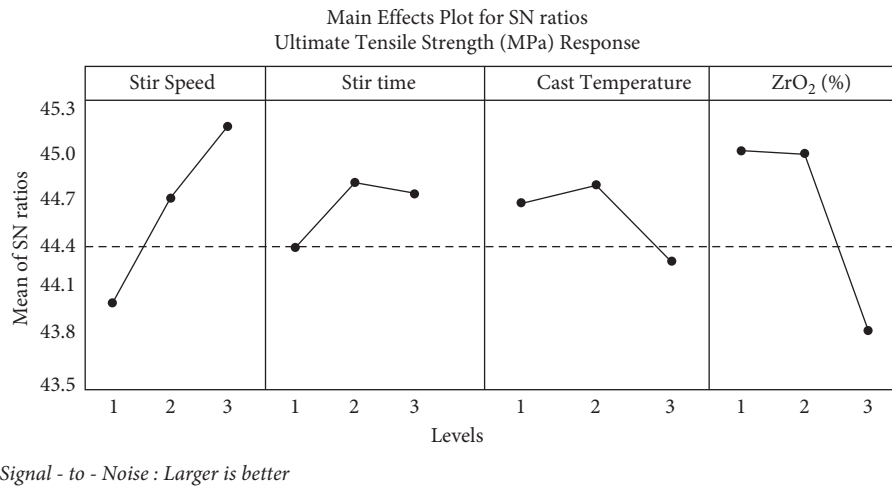


FIGURE 4: Main effect plot for ultimate tensile strength.

change at all. It is possible that the porosity or voids caused by clustered ZrO₂ particles reduces the value of UTS, which diminishes the advantages of reinforcing particles beyond the critical limit of reinforcement. Centrifugal currents are set up in an aluminium melt when the stirring speed is increased, resulting in a vortex. To increase the composites' UTS, this aids in dispersing the reinforcing particles evenly throughout the melt. The formation of a vortex by stirring speed and time is critical to the distribution of reinforced particles in an aluminium matrix. Because vortex have a greater ability to draw in air, prolonged stirring time results in composite porosity. The aluminium melt's viscosity and gas pick-up are influenced by the cast temperature. Low viscosities caused by low casting temperatures generally have difficulties stirring aluminium melt, while high viscosities lose control over particle movement, making it difficult to distribute particles uniformly throughout composites. As an example, value stating that zirconium oxide reinforcement accounted for more than any other factor. For a higher ultimate tensile strength, stir-casting conditions A3B2C2D2, which include a 600 rpm stir speed, an 8-minute stir period, and ZrO₂ weight

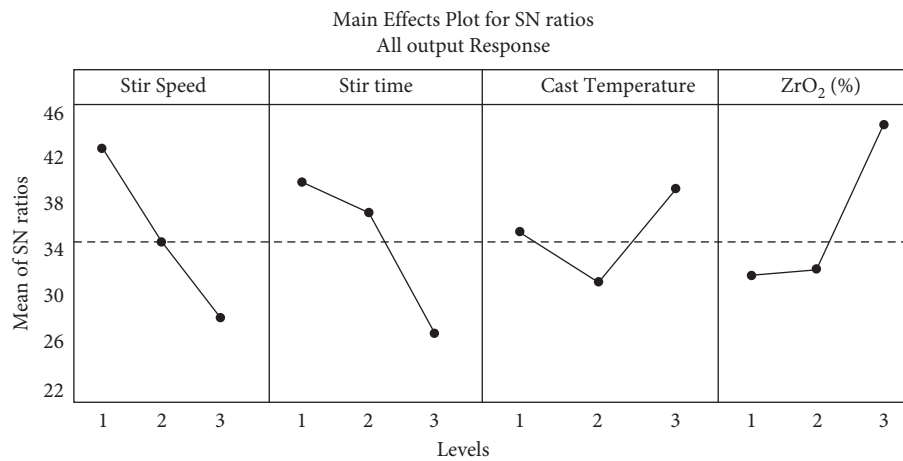
percentage of 10%, should be used instead. The Taguchi L9 trials were the ideal sets for maximising UTS, which founded as optimum.

3.1.4. *Optimization of Stir-Casting Process.* Using the Taguchi method, it was not possible to simultaneously optimise many outputs due to limitations. Using a multi-objective optimization approach, WL was minimised while UTS and hardness are maximised using the stir-cast method. Based on the measured experimental results, the S/N ratio data is calculated (refer Table 2). The S/N ratio data of each response were used to assign a rank to each response. The top rank is given to the S/N ratio with the highest value, followed by the second and so on (refer to Table 4). Figure 5 shows the Main effect plot for responses of Signal to Noise ratio.

3.1.5. *Confirmation Experiments.* Table 5 shows the progress of Stir casting through Anova output results. Experiment results for the beginning and ideal conditions are shown in Table 6 and Figure 6 shows the contribution of parameters to

TABLE 4: Super ranking concept: stir-casting progression result summary.

Trial. No	S/N ratio, dB			Rank			Squaring rank			Sum of squared rank
	Hardness (Hv)	Ultimate tensile strength (MPa)	WL	Hardness (Hv)	Ultimate tensile strength (MPa)	WL	Hardness (Hv)	Ultimate tensile strength (MPa)	WL	
L1	36.10	44.23	-22.80	7	7	7	49	49	49	147
L2	36.18	44.92	-22.21	5	4	4	25	16	16	57
L3	35.82	43.01	-23.58	9	9	9	81	81	81	243
L4	36.07	43.72	-23.35	8	8	8	64	64	64	192
L5	36.46	44.84	-22.41	3	5	5	9	25	25	59
L6	36.50	45.11	-20.09	2	2	2	4	4	4	12
L7	36.24	45.02	-21.73	4	3	3	16	9	9	34
L8	36.16	44.60	-22.48	6	6	6	36	36	36	108
L9	36.52	45.94	-18.89	1	1	1	1	1	1	3



Signal - to - Noise : Smaller is better

FIGURE 5: Main effect plot for responses of signal to noise ratio.

different responses. Note that the Taguchi technique was utilised to discover ideal conditions for stir-casting progression for a distinct response, but the SRC technique was utilised to find the optimum parameters for several reactions. Hardness, wear loss, and UTS were enhanced by 6.58%, 37.68%, and 29.26% using the Taguchi method, respectively. SRC yielded a 37.68% reduction in WL, a 25.02% increase in UTS, and a 5.64% increase in hardness associated with the starting experimental conditions of the stir-casting method. The better findings show that Taguchi and SRC are effective.

3.2. Hot-Pressing Technique. Stir-cast composite samples benefit from improved characteristics thanks to the use of the hot-pressing process (prepared as per optimized condition). SRC found the best results with a ZrO₂ reinforcement weight of 10% in an Al 7075-ZnO matrix. Consequently, the hot-pressing procedure was used on the Al 7075/ZnO and ZrO₂ specimens that had been stir-casted. By applying hot-press techniques with diverse sets of parameters, the WL, hardness, and ultimate tensile strength were studied. For hot-press, Taguchi L9 experiments were conducted to acquire the experimental input-output data.

Table 7 shows the S/N ratio based on experimental results. Pareto analysis of variance was utilized to determine the impacts of hot-press factors and the ideal level. Table 8 summarises the hot-pressing technique's findings.

3.2.1. Effect of Hardness Factors. Figure 7 explains hot-pressing parameters affect the hardness of the material. As pressure was raised, the hardness values rose in a straight line. Full densification, which leads to higher hardness values, may be achieved by applying pressure to composite samples. Low temperatures allow composites to solidify prematurely before pressure is applied, whereas high temperatures produce significant grain growth and low hardness values as a result of the cooling process. Maximum time below pressure is constantly preferred to achieve full compaction and hence higher hardness values. Compared to pressure and temperature, dwell time or holding time has a negligible effect on hardness. The three most significant factors were found to be 69.08 % pressure, 19.47 % temperature, and 11.46 % dwell duration (refer to Table 8). Temperature, pressure, and dwell time at 400°C, 100 MPa, and 40 minutes were found to be the ideal hot pressing conditions for maximizing hardness values.

TABLE 5: Stir-casting progression: pareto ANOVA output results.

Parameters	Levels	Stirring speed	Stirring time	Casting temperature	ZrO ₂ %	Total
Mean	1	42.06	39.88	25.32	29.44	103.23
Factor	2	34.22	37.07	30.11	29.11	—
Levels	3	26.95	26.28	37.92	44.68	—
MSD		344.72	307.28	95.23	474.16	1221.39
% contribution		28.07	25.31	8.72	37.90	100
Optimum levels		A3B3C2D2(not at L18 experiments combination)				

TABLE 6: Validation of experimental outcome for optimum settings of stir-casting progression.

State	Stir-casting state	Responses	% Improvement
Optimum setting for hardness	Stirring speed: 575 rpm	Hardness: 68	6.58%
	Stirring time: 15 min	—	—
	Casting temperature: 740°C	—	—
	ZrO ₂ wt.%: 4% wt	—	—
Optimum setting for wear loss	Stirring speed: 625 rpm	WL: 8.6 g	37.68%
	Stirring time: 15 min	—	—
	Casting temperature: 740°C	—	—
	ZrO ₂ wt.%: 8% wt	—	—
Optimum setting for UTS	Stirring speed: 625 rpm	UTS: 210.3 MPa	29.26%
	Stirring time: 10 min	—	—
	Casting temperature: 740°C	—	—
	ZrO ₂ wt.%: 8% wt	—	—
Optimum setting for all outputs	Stirring speed: 600 rpm	WL: 8.6 g	WL: 37.68%
	Stirring time: 12 min	UTS: 204.2 MPa	UTS: 25.02%
	Casting temperature: 740°C	Hardness: 68.1	UTS: 25.02%
	ZrO ₂ wt.%: 8% wt	—	—

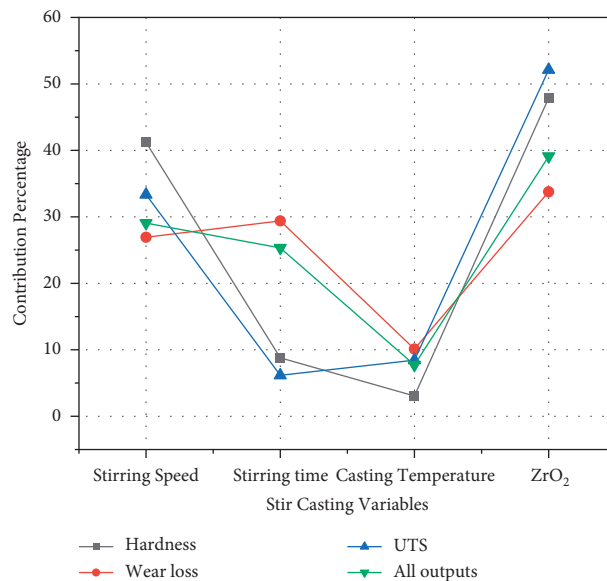


FIGURE 6: Contribution of parameters on variant responses in percentage.

3.2.2. *Effect of Wear Loss Factors.* As shown in Figure 8, hot-pressing circumstances have a significant impact on wear loss. Low wear loss can be attributed to high pressure and a shorter dwell duration. To optimise heat transmission, grain structure, and pore closure in pressurised composites, metal is forced closer to the die surface walls

by increased pressure. The least amount of wear is found when the temperature is maintained at a consistent intermediate range. An early solidification and lower heat extraction capabilities result in minimal wear loss. Pressure, temperature, and dwell time are identified to contribute 48.77%, 38.07%, and 13.17% to wear loss,

TABLE 7: Hot-pressing progression’s experimental input and output setting.

Trial. No.	Input			Output				S/N ratio, dB	
	Temperature(E)	Pressure(F)	Dwelling time	Hardness	Ultimate tensile strength	Wear loss	Hardness	Ultimate tensile strength	Wear loss
L1	420	40	15	70.2	216.1	8.4	36.93	46.69	-18.49
L2	420	80	30	72.3	233.6	7.5	37.18	47.37	-17.50
L3	420	120	45	72.7	236.5	7.1	37.23	47.48	-17.03
L4	460	40	30	71.7	227.5	8.0	37.11	47.14	-18.06
L5	460	80	45	72.8	239.1	6.6	37.24	47.57	-16.39
L6	460	120	15	73.3	241.9	5.2	37.30	47.67	-14.32
L7	500	40	45	70.6	220.9	8.3	36.98	46.88	-18.38
L8	500	80	15	71.3	233.4	7.9	37.06	47.36	-17.95
L9	500	120	30	72.3	228.9	8.2	37.18	47.19	-18.28

TABLE 8: Hot-pressing progression’s Pareto ANOVA results.

Output	Parameters	Levels	E (°C)	F (MPa)	G (min)	Total
Hardness (Hv)	Mean	1	37.20	37.11	37.16	111.59
	Factor	2	37.25	37.19	37.21	—
	Levels	3	37.15	37.29	37.23	—
	MSD		0.015	0.048	0.008	0.071
	% Contribution		18.47	69.09	12.47	100
	Optimum levels			E2F3G3 (not at L9 assortment)		
Wear loss	Mean	1	-17.67	-18.31	-16.92	-52.13
	Factor	2	-16.26	-17.28	-17.95	—
	Levels	3	-18.20	-16.54	-17.27	—
	MSD		07.08	03.73	01.64	12.44
	% Contribution		49.76	36.07	14.18	100.00
	Optimum levels			E2F3G1		
Ultimate tensile strength (Mpa)	Mean	1	47.18	46.91	47.24	141.79
	Factor	2	47.46	47.43	47.23	—
	Levels	3	47.15	47.45	47.31	—
	MSD		0.19	0.56	0.02	0.77
	% Contribution		24.54	74.08	1.38	100
	Optimum levels			E2F3G3 (not the combination of L9 experiments)		

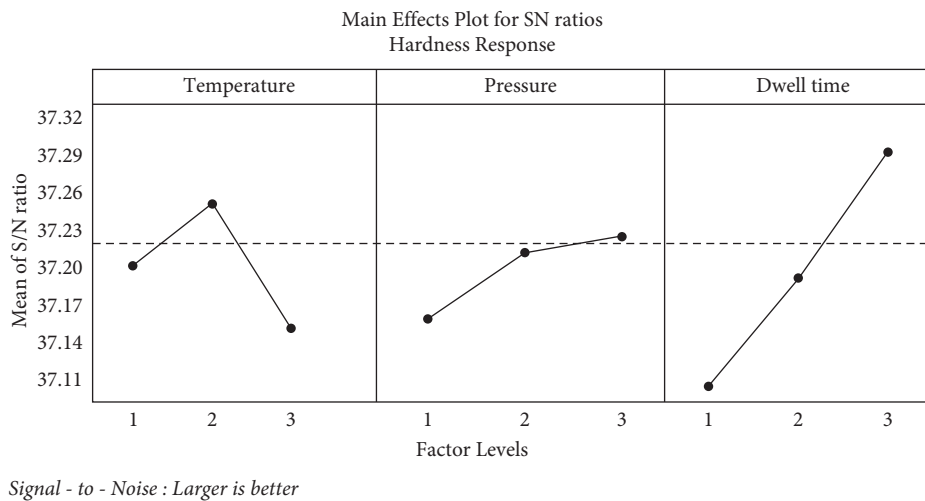


FIGURE 7: Main effect plot for ultimate tensile strength.

respectively. The optimum conditions (E2F3G1: 480°C, 100 MPa, and a dwell time of 20 minutes) result in the least amount of wear and tear.

3.2.3. *Effect of Ultimate Tensile Strength Factors.* Figure 9 depicts the UTS, which follows the same pattern as the values of hardness and Figure 10 shows the mean for overall output

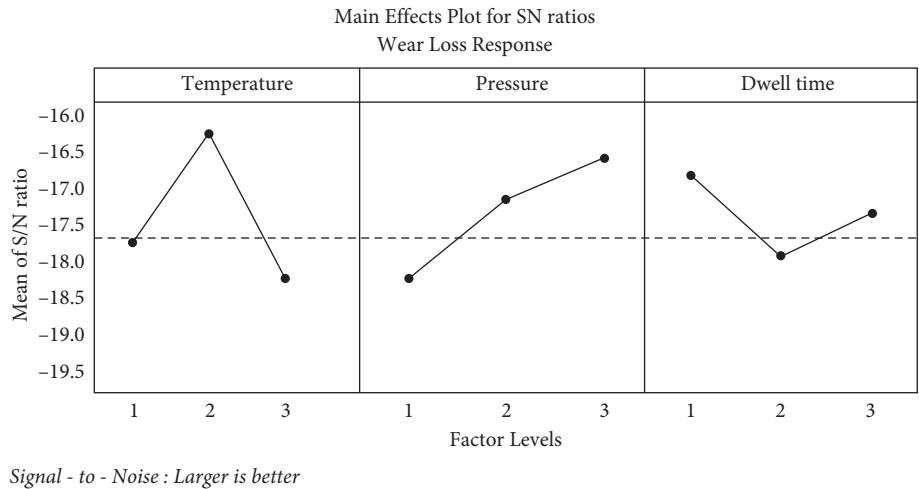


FIGURE 8: Main effect plot for wear loss responses.

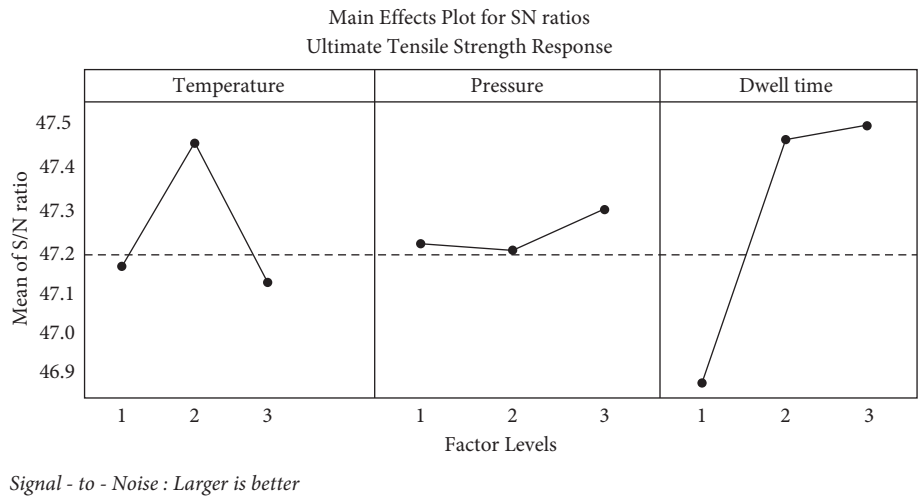


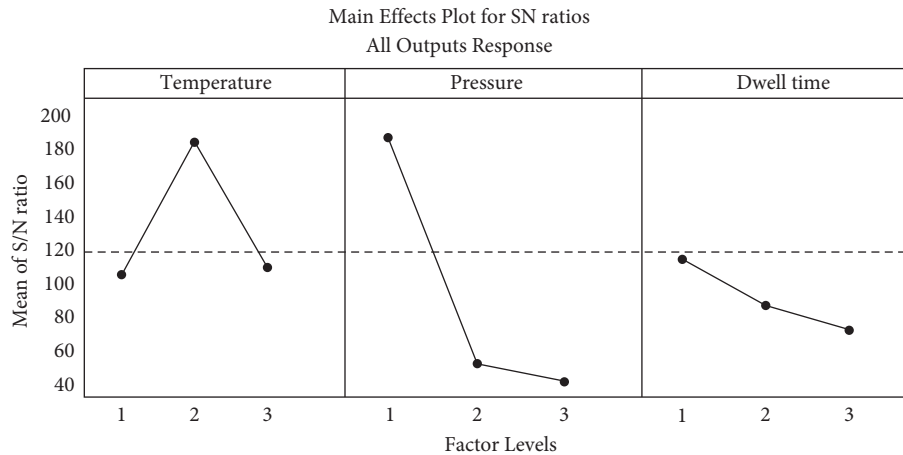
FIGURE 9: Main effect plot for wear loss.

responses. Figure 11 shows that hardness and ultimate tensile strength have a high link, which may explain why this is the case. There was no discernible increase in characteristics due to an increase in pressurization pressure after reaching the midpoint. When the temperature was kept in the medium range and the dwell time was increased, composites' ultimate tensile strength improved. A total of 75.09%, 1.39%, and 23.52% was provided by pressure, dwell time, and temperature. It was observed that E2F3G3 was the ideal combination of factors and levels to maximise the UTS of the composite.

3.2.4. Optimization of Hot-Pressing Process. Controversial comments can be prioritized using the “super ranking” idea. For hot-pressing conditions, the processes in the super ranking concept are similar to those for stir-cast conditions, and outcomes are exposed in Table 9. For higher-quality composites, the ideal hot-pressing settings were found to be E2F3G3 (440°C, 100 MPa, and a 40 minute dwell period). There was a maximum contribution of 73.18%, followed by a

dwell time of 4.35% for pressure and temperature, respectively. For each individual output, the percentage involvement and ideal factor level were identified to be varied, which may be attributed to an input factor impact on the outcome of each individual. Individual outputs, as well as several outputs, have different optimal variables and levels than those found in L9 trials, according to research.

3.2.5. Experiments for Confirmation. Pareto output results for all the outputs were given in Table 10. Comparing outcomes of the starting and ideal hot-pressing experiments is shown in Table 11. Using the Taguchi method, a rise of 4.7% in hardness and a 13.05% increase in UTS were found (refer Table 11). An increase of 42.9% was achieved by creating the ideal circumstances to minimize wear (refer Table 11). The ideal circumstances for SRC resulted in a 39.29% decrease in WL, while an 11.54% rise in UTS and a 4.88% increase in hardness, respectively, were found (refer to Table 11). It is possible to conduct optimization work using Taguchi and SRC. Figure 12 shows the contribution of percentage at different parameters.



Signal - to - Noise : Smaller is better

FIGURE 10: Main effect plot for responses of signal to noise ratio.

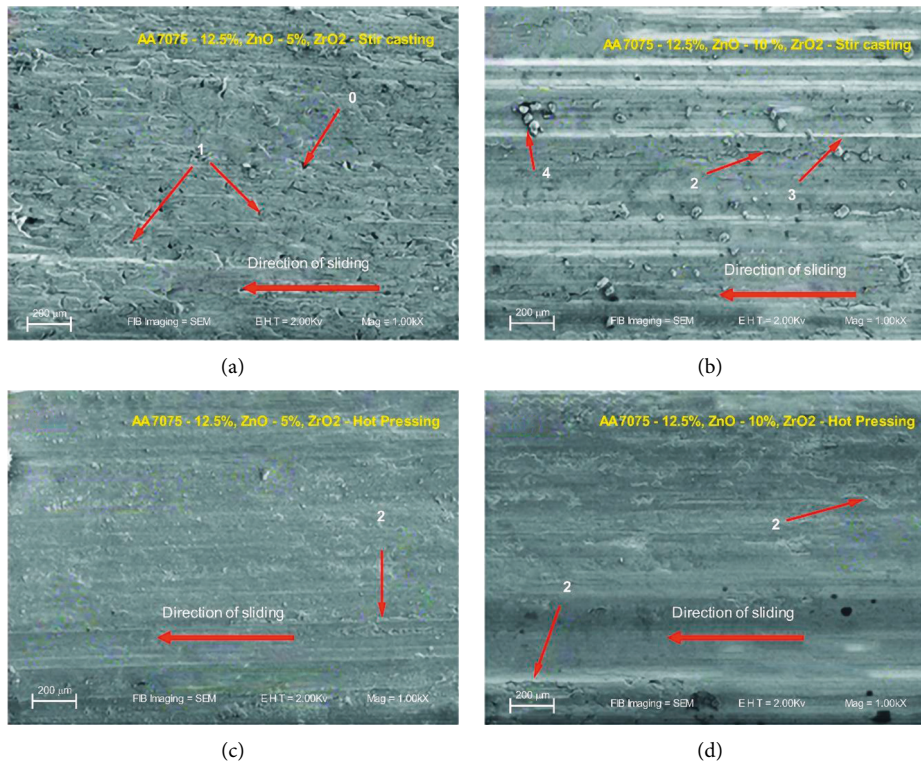


FIGURE 11: Wear Surface morphology of hot-pressed and stir-casting AA 7075/ZnO-ZrO₂ composites. (a) AA7075-12.5%, ZnO-5%, ZrO₂-stir casting. (b) AA7075-12.5%, ZnO-10%, ZrO₂-stir casting. (c) AA7075-12.5%, ZnO-5%, ZrO₂-hot pressing. (d) AA7075-12.5%, ZnO-10%, ZrO₂-hot pressing.

3.3. Hot-Pressing and Stir-Casting Comparison. Stir-cast and hot-press processes have been compared in Table 12 for their optimized qualities. The stir-casting process was used to create composites for hot-pressing under optimised parametric conditions. In comparison to the stir-casting process, the hot-pressing technique reduced WL by 40.8% while increasing UTS and hardness values by 19.83% and 9.6%, respectively.

3.4. Microstructure Characterisation. Figure 13 shows the microstructural characterization of Al 7075/ZnO-ZrO₂ composites made by stir-casting and hot-pressing. The surface morphology of ZrO₂ particles was studied using optical and SEM micrographs. ZrO₂ particles are similar in appearance to these bright silvery, almost spherical particles. Al 7075/ZnO-5% ZrO₂ and ZnO-10% ZrO₂ in stir-casted conditions are shown in Figures 13(a)–13(d). A dendritic

TABLE 9: Super ranking concept's result summary.

Trial No	S/N ratio, dB			Ranking			Square ranking			Sum of squared rank
	Hardness	Ultimate tensile strength	Wear loss	Hardness	Ultimate tensile strength	Wear loss	Hardness	Ultimate tensile strength	Wear loss	
L1	36.93	46.69	-18.49	9	9	9	81	81	81	243
L2	37.18	47.37	-17.50	4	4	4	16	16	16	48
L3	37.23	47.48	-17.03	3	3	3	9	9	9	27
L4	37.11	47.14	-18.06	6	7	6	36	49	36	121
L5	37.24	47.57	-16.39	2	2	2	4	4	4	12
L6	37.30	47.67	-14.32	1	1	1	1	1	1	3
L7	36.98	46.88	-18.38	8	8	8	64	64	64	192
L8	37.06	47.36	-17.95	7	5	5	49	25	25	99
L9	37.18	47.19	-18.28	4	6	7	16	36	49	101

TABLE 10: Pareto ANOVA outcome for all outputs.

Parameters	Levels	E (°C)	F (MPa)	G (min)	Total
Mean	1	106	185.33	115	282
Factor	2	45.33	53	90	—
Levels	3	130.67	43.68	78	—
MSD		11570.67	37668.67	2238	51447.30
% contribution		23.49	72.18	4.34	100
Optimum levels		E2F3G3 (not the combination of L9 experiments)			

TABLE 11: Validation experimental outcome for optimum settings of hot-pressing progression.

Setting	Hot-pressing progression	Response	% Improvement
Primary (Table 7)	Temperature: 420°C	WL: 8.5 g	—
	Pressure: 40 MPa	UTS: 216.2 MPa	—
	Dwell time: 15 min	Hardness: 70.3	—
Optimum setting for hardness	Temperature: 460°C	Hardness: 73.5	4.7%
	Pressure: 120 MPa	—	—
	Dwell time: 45 min	—	—
Optimum setting for wear loss	Temperature: 460°C	WL: 4.8 g	42.9%
	Pressure: 120 MPa	—	—
	Dwell time: 15 min	—	—
Optimum setting for UTS	Temperature: 460°C	UTS: 244.3 MPa	13.05%
	Pressure: 120 MPa	—	—
	Dwell time: 45 min	—	—
Optimum setting for all outputs	Temperature: 460°C	WL: 5.1 g	WL: 39.29%
	Pressure: 120 MPa	UTS: 244.3 MPa	UTS: 11.54%
	Dwell time: 45 min	Hardness: 74.5	Hardness: 4.91%

structure can be seen in Figures 13(a)–13(d) that grows in accordance with beneficial growth patterns. A columnar shape is influenced by the direction of heat flow in grains, which promotes the growth of some grains while inhibiting the growth of others. Figures 13(a)–13(d) depict the ZrO₂ particle dispersion in the Al 7075/ZnO matrix. The majority of ZrO₂ particles have a spherical shape. Additionally, the ZnO/Al 7075 alloy has a strong interfacial interaction with ZrO₂, which assists in achieving improved mechanical properties. Al 7075/ZnO-10% ZrO₂ composites S1-HT (Al 7075/ZnO) and S2-HT (Al 7075/ZnO) in hot-pressing conditions are shown in Figures 13(e)–13(h). To create a

composite with good mechanical properties, the ZrO₂ reinforcement particles must be evenly distributed in the matrix alloy. If high pressure and hot pressing had been used, the lack of porosity and grain refinement in the composites would have indicated solid castings. ZrO₂ particle surface homogeneity is discovered. As shown in Figures 13(e)–13(h), the ZrO₂ particles are dispersed uniformly throughout the Al 7075/ZnO matrix. The mechanical properties of composites can be improved by having a more uniform dispersion of the matrix and the reinforcement. Al 7075/ZnO-ZrO₂ composites are examined by energy dispersive X-ray spectroscopy.

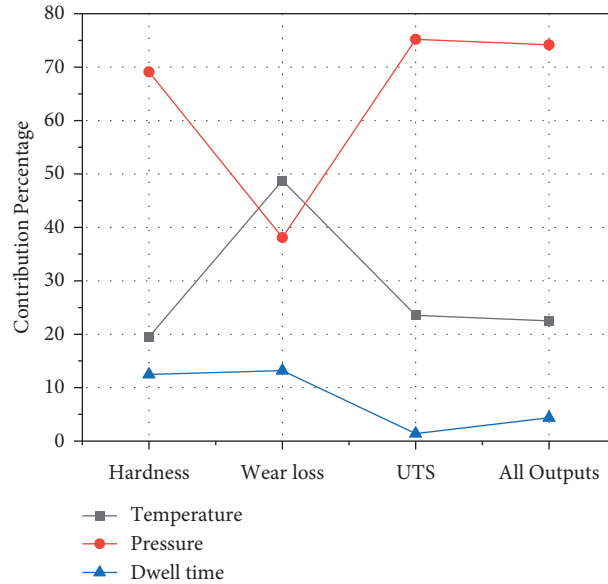


FIGURE 12: Hot-pressing constraint's percentage of contribution.

TABLE 12: Evaluation of Variant processing methodology Characteristics.

Optimal characteristics of variable processes		Improvement percentage (%)
Stir cast	Hot press	
WL: 8.7 g	WL: 5.2 g	40.80
Ultimate tensile strength: 204.2 MPa	Ultimate tensile strength: 244.3 MPa	19.83
Hardness: 68.1	Hardness: 74.5	09.60

3.5. Wear Surface Morphology. Figure 11 depicts the wear patterns of Al 7075/ZnO-ZrO₂ composites made using the stir-casting and hot-press conditions described above. From Figure 11, 2 indicates a delaminated area, 3 indicates dense, narrow abrasive grooves, 4 indicates debris, and 5 indicates an abrasion area. For Al 7075/ZnO-ZrO₂ composites exposed to stir cast Figures 11(a) and 11(b), hot pressing Figure 11(c), wear tracks had different wear profiles. These findings support the notion that abrasion wear has undergone a significant mechanism of wear change. In contrast to the Al 7075/ZnO-ZrO₂ composites surface exposed to the hot press and displays slim abrasive groove, less debris, and slight abrasive areas; a huge amount of delaminated areas, holes, and abundant grooves had been detected on the AA 7075-12.5% ZnO-ZrO₂ composite surface exposed to stir casting. Figure 11(a) indicates that the stir-cast S1 composite (Al 7075/ZnO-5% ZrO₂) has a higher degree of plastic deformation because of the impression of the pin and disc at maximum load. Observed maximum wear loss is substantially supplemented by achieved results, namely maximum wear loss at 30 N, with the width of the wear grooves. Table 13 shows the Validation experimental results for optimum settings for stir-casting process.

A small amount of plastic deformation can be seen in the stir-cast S2 composite (Al 7075/ZnO-10% ZrO₂) at the load of 30 N, as shown in the micrograph of Figure 11(b).

Wear grooves are narrower with a lower wear loss of 8.7 g and a higher VHN hardness of 67.4; these findings are supported by the obtained results, which indicate negligible wear loss under a 30 N load. S2 composites, in contrast to S1 composites, include more hard and ceramic particles. Wear can be reduced by using ceramic elements as load-carrying material. Many researchers found the same thing. Hot-pressed S1-HP composite (Al 7075/ZnO-10% ZrO₂) reveals a slight abrasion region (Figure 11(c)), which is corroborated by SEM microscopy. Figure 11(c) shows that the wear groove widths are smaller than in Figures 11(a) and 11(b), with a nominal wear loss of 8.4 g. A higher hardness of 69.8 VHN, as opposed to that made by means of the stir-casting processes, could also account for improved wear resistance. In addition, samples produced by simultaneously applying high pressure and a lower dwell period result in low wear losses. As shown in Figure 11(c), the wear track surface had many slim and narrow grooves similar to the sliding track and some wear debris elements, which indicates mild abrasive wear. As shown in Figure 11(d), the SEM micrograph exhibits like surface to S1-HP composite. For comparison, the wear tracks in Figure 11(d) indicate the least wear loss of 5.1 grams in comparison to Figures 11(a)–11(c). Compared to other composites, the 73.8 VHN hardness and grain refinement because of the hot press may be a factor in the improved wear rate of hot-pressed carbon fibre.

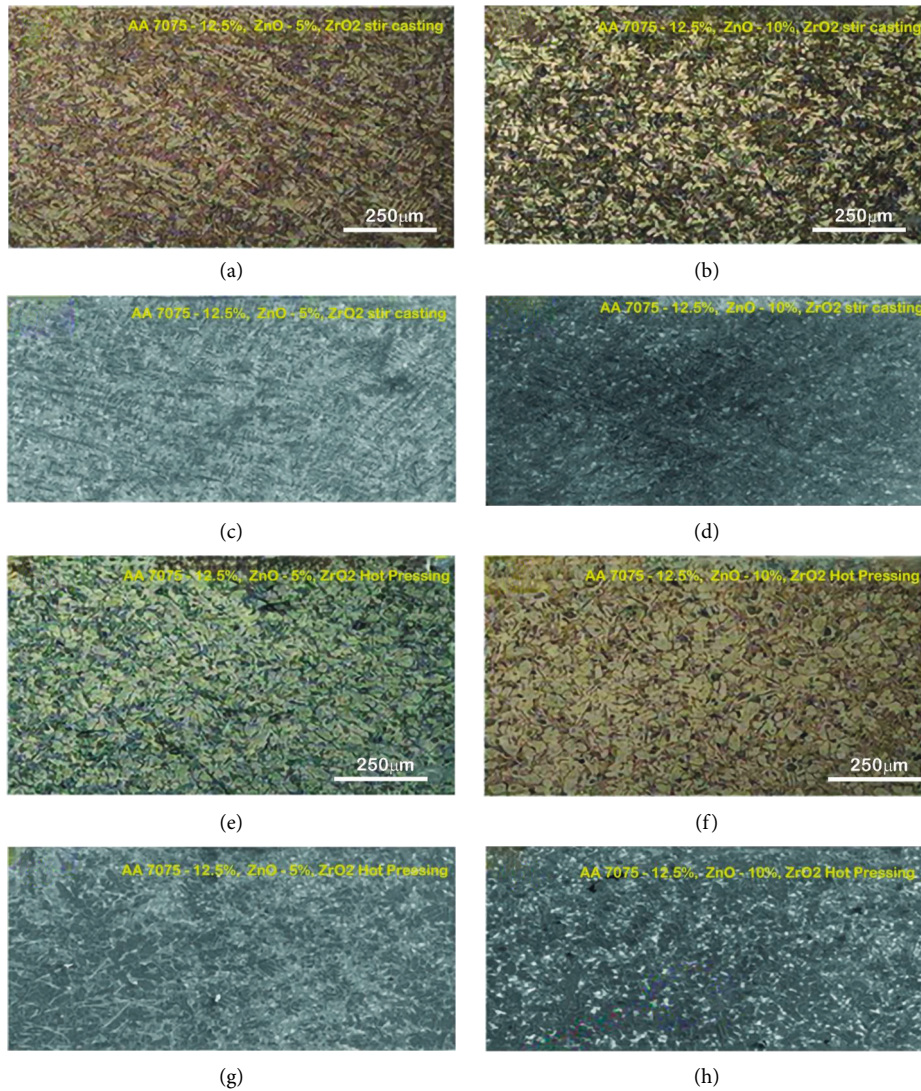


FIGURE 13: Microstructure of hot-pressed and stir-casting AA 7075/ZnO-ZrO₂ composite. (a, c) AA7075-12.5%, ZnO-5%, ZrO₂ stir casting. (b, d) AA7075-12.5%, ZnO-10%, ZrO₂ stir casting. (e, g) AA7075-12.5%, ZnO-5%, ZrO₂ hot pressing. (f, h) AA7075-12.5%, ZnO-10%, ZrO₂ hot pressing.

TABLE 13: Validation experimental outcome for optimum settings for stir-casting progression.

State	Processing parameters	Response	Composite specification
Primary	Stirring speed: 525 rpm	WL: 13.8 g	S1 (Al 7075/ZnO-5% ZrO ₂)
	Stirring time: 5 min	UTS: 162.7 MPa	—
	Casting temperature: 700°C	Hardness: 63.8	—
	ZrO ₂ wt. %: 4	—	—
Optimum setting for all outputs	Stirring speed: 625 rpm	WL: 8.5 g	S2 (Al 7075/ZnO-10% ZrO ₂)
	Stirring time: 15 min	UTS: 204.2 MPa	—
	Casting temperature: 740°C	Hardness: 68.1	—
	ZrO ₂ wt. %: 8% wt	—	—
Initial hot pressing	Temperature: 420°C	WL: 8.5 g	S1-HP (Al 7075/ZnO-10%ZrO ₂)
	Pressure: 40 MPa	UTS: 217.2 MPa	—
	Dwell time: 15 min	Hardness: 70.3	—
Hot pressing optimum setting for all outputs	Temperature: 460°C	WL: 5.2 g	S2-HP (Al 7075/ZnO-10%ZrO ₂)
	Pressure: 120 MPa	UTS: 244.3 MPa	—
	Dwell time: 45 min	Hardness: 74.5	—

4. Conclusions

Using a two-step procedure, which includes stir-casting and hot-pressing processes, the current work conserves natural resources while also healing or fixing cast faults. The following are some observations on the acquired results: [41–43].

- (1) Al 7075/ZnO composites reinforced with ZrO₂ at different weight percentages can be made via stir casting. Casting properties were most strongly influenced by ZrO₂ reinforcements, succeeded by stirring speed, stirring time, and temperature.
- (2) When the best stir-casting circumstances were determined, wear loss was reduced by 37.68% (13.8–8.4 g), 25.02%, and 5.64%, respectively, compared to the first stir-casting parameters, and hardness was increased by 63.8–67.4% compared to the original conditions. For stir casting, a Pareto analysis of variance found optimum conditions, which were not found in a set of L9 investigations, and their related properties show that the models constructed and analysis done were effective.
- (3) A hot-pressing process is used to repair or decrease pores in samples that have been manufactured under stir-cast optimized conditions. Variables (such as temperature, pressure, and dwell time) that affect characteristics (such as wear loss, UTS, and hardness) during hot pressing have been experimentally investigated. Pressure, temperature, and dwell time all have a role in sealing pores, which results in enhanced characteristics.
- (4) Wear loss was reduced by 39.29%, UTS increased 11.54%, and hardness values increased 4.88% as compared to the initial hot-pressing circumstances, according to the super ranking idea.
- (5) The hot-pressing process used on the improved stir-cast components reduced wear loss by 40.8%, increased UTS by 19.83%, and increased hardness by 9.6%. Because of the results obtained, even stir-cast optimised condition have a greater possibility to enhance the characteristics when subjected to hot press.

Data Availability

The authors confirm that all the data are available in this research article.

Conflicts of Interest

The authors declare that they have no conflicts of interest.

References

- [1] R. H. Oskouei, M. R. Barati, and R. N. Ibrahim, "Surface characterizations of fretting fatigue damage in aluminum alloy 7075-T6 clamped joints: the beneficial role of Ni-P coatings," *Materials*, vol. 9, no. 3, pp. 141–3, 2016.
- [2] R. P. Udayagiri, S. B. Koppad, P. G. Gupta, M. Munishamaiah, K. Bontha, and S. Bontha, "The effect of heat treatment on the mechanical and tribological properties of dual size SiC reinforced A357 matrix composites," *Journal of Materials Research and Technology*, vol. 9, no. 3, pp. 6434–6452, 2020.
- [3] F. Bedir, "Characteristic properties of Al-Cu-SiCp and Al-Cu-B4Cp composites produced by hot pressing method under nitrogen atmosphere," *Materials & Design*, vol. 28, no. 4, pp. 1238–1244, 2007.
- [4] J. Hashim, L. Looney, and M. S. J. Hashmi, "Metal matrix composites: production by the stir casting method," *Journal of Materials Processing Technology*, vol. 92–93, no. 93, pp. 1–7, 1999.
- [5] D. Bommana, T. R. K. Dora, N. P. Senapati, and A. S. Kumar, "Effect of 6 Wt.% particle (B4C + SiC) reinforcement on mechanical properties of AA6061 aluminum hybrid MMC," *Silicon*, vol. 14, no. 8, pp. 4197–4206, 2022.
- [6] R. Srinivasan, B. Suresh Babu, P. Prathap, R. Whenish, R. Soundararajan, and G. Chandramohan, "Optimization of friction stir welding process parameters on AA 6063-SiC-B4C hybrid metal matrix composites by genetic algorithm," *Journal of Ceramic Processing Research*, vol. 22, no. 1, pp. 16–24, 2021.
- [7] H. Xin, Y. Lu, L. Chen et al., "Heat propagation simulation of thin-walled Ti6Al4V alloy components fabricated by double-wire GTAW additive manufacturing," *Science and Technology of Welding & Joining*, vol. 27, no. 6, pp. 446–454, 2022.
- [8] B. Prasanna Nagasai, S. Srikanth, and J. A. Ranga Babu, "Mechanical properties of AA 7075-nano ZrO₂ reinforced matrix composites," *Advances in Applied Mechanical Engineering*, Springer, Berlin, Germany, pp. 921–928, 2020.
- [9] S. E. Hernández-Martínez, J. J. Cruz-Rivera, C. G. Garay-Reyes, and J. L. Hernández-Rivera, "Experimental and numerical analyses of the consolidation process of AA 7075–2 wt.% ZrO₂ powders by equal channel angular pressing," *Journal of Materials Engineering and Performance*, vol. 28, no. 1, pp. 154–161, 2019.
- [10] M. Kaseem, Y. H. Lee, and Y. G. Ko, "Incorporation of MoO₂ and ZrO₂ particles into the oxide film formed on 7075 Al alloy via micro-arc oxidation," *Materials Letters*, vol. 182, pp. 260–263, 2016.
- [11] A. Shanmugasundaram, "Experimental investigation of mechanical and tribological properties of Al 7075-MoS₂/ZrO₂/Ni hybrid composite," *Advances in Materials and Metallurgy*, Springer, Berlin, Germany, 2019pp. 299–309, Lecture Notes in Mechanical Engineering.
- [12] M. Feng, Y. Liao, M. Chen, S. Zhu, and F. Wang, "Crystallization and thermal shock behaviors of SiO₂-Al₂O₃-ZnO-CaO-based glass with added different contents of CeO₂ at 900°C," *Cailiao Yanjiu Xuebao/Chinese Journal of Materials Research*, vol. 36, no. 2, pp. 90–98, 2022.
- [13] F. C. R. Hernandez, J. M. H. Ramirez, and R. Mackay, *Al-Si Alloys: Automotive, Aeronautical, and Aerospace Applications*, 2017.
- [14] A. Lakshmikanthan, S. Bontha, M. Krishna, P. G. Koppad, and T. Ramprabhu, "Microstructure, mechanical and wear properties of the A357 composites reinforced with dual sized SiC particles," *Journal of Alloys and Compounds*, vol. 786, pp. 570–580, 2019.
- [15] R. Piya, S. Krishnan, P. K. Muraliraja et al., "Optimization of stir-squeeze casting parameters for production of metal matrix composites using a hybrid analytical hierarchy

- process-Taguchi-Grey approach,” *Engineering Optimization*, vol. 52, no. 7, pp. 1166–1183, 2020.
- [16] N. Barati, J. Jiang, and E. I. Meletis, “Microstructural evolution of ceramic nanocomposites coated on 7075 Al alloy by plasma electrolytic oxidation,” *Surface and Coatings Technology*, vol. 437, Article ID 128345, 2022.
- [17] S. Gangwar, P. Arya, and V. K. Pathak, “Optimal material selection for ship body based on fabricated zirconium dioxide/silicon carbide filled aluminium hybrid metal alloy composites using novel Fuzzy based preference selection index,” *Silicon*, vol. 13, no. 8, pp. 2545–2562, 2021.
- [18] A. N. Tiwari, V. Gopinathan, and P. Ramakrishnan, “Processing of modified ai (7010)-sic particulate composites by mechanical alloying and hot-pressing,” *Materials and Manufacturing Processes*, vol. 6, no. 4, pp. 621–633, 1991.
- [19] M. Shahedi Asl, M. Ghassemi Kakroudi, B. Nayebi, and H. Nasiri, “Taguchi analysis on the effect of hot pressing parameters on density and hardness of zirconium diboride,” *International Journal of Refractory Metals and Hard Materials*, vol. 50, pp. 313–320, 2015.
- [20] V. Sivamaran, V. Balasubramanian, M. Gopalakrishnan, V. Viswabaskaran, and A. G. Rao, “Combined synthesis of carbon nanospheres and carbon nanotubes using thermal chemical vapor deposition process,” *Chemical Physics Impact*, vol. 4, Article ID 100072, 2022.
- [21] C. N. Chakravarthy and S. Sathees Kumar, “Surface roughness measurement on Al-7075 reinforced with the ZrO₂ powder by using box-behnken analysis,” *International Journal of Mechanical and Production Engineering Research and Development*, vol. 10, no. 2, pp. 859–866, 2020.
- [22] A. Singh Rathaur, J. Kumar Katiyar, and V. Kumar Patel, “Experimental analysis of mechanical and structural properties of hybrid aluminium (7075) matrix composite using stir casting method,” *IOP Conference Series: Materials Science and Engineering*, vol. 653, no. 1, Article ID 012033, 2019.
- [23] V. B. Nathan, R. R.Soundararajan, C. B. Abraham, and F. Rahman.A, “Evaluation of mechanical and metallurgical properties on aluminium hybrid metal matrix composites,” *Materials Today Proceedings*, vol. 18, pp. 2520–2529, 2019.
- [24] P. N. Bellamkonda, “Wear and electrochemical corrosion behaviour of nano ZrO₂ reinforced AA7075 metal matrix composites,” *International Journal of Mechanical and Production Engineering Research and Development*, vol. 9, no. 3, pp. 793–802, 2019.
- [25] S. Venkatesan, B. Visvalingam, G. Mannathusamy, V. Viswanathan, and A. G. Rao, “Effect of chemical vapor deposition parameters on the diameter of multi-walled carbon nanotubes,” *International Nano Letters*, vol. 8, no. 4, pp. 297–308, 2018.
- [26] F. Zhu, Y. Jin, B. Ji et al., “CuO/ZrO₂ co-promoted by ZnO, Sn, and CuP shows high efficiency for dimethyldichlorosilane production in the Rochow-Müller reaction,” *Applied Catalysis A: General*, vol. 636, Article ID 118582, 2022.
- [27] J. S. Midala, I. H. Kamari, H. M. Al-Hada et al., “Effect of calcination temperature on the structural and optical properties of (ZnO)_{0.8} (ZrO₂)_{0.2} nanoparticles,” *Journal of Inorganic and Organometallic Polymers and Materials*, vol. 32, no. 5, pp. 1755–1765, 2022.
- [28] X. Shi, X. Chen, Z. Xu et al., “Efficient conversion of benzene and syngas to toluene and xylene over ZnO-ZrO₂&H-ZSM-5 bifunctional catalysts,” *Chinese Journal of Chemical Engineering*, vol. 45, pp. 203–210, 2022.
- [29] J. Ding, Z. Li, W. Xiong, Y. Zhang, A. Ye, and W. Huang, “Structural evolution and catalytic performance in CO₂ hydrogenation reaction of ZnO-ZrO₂ composite oxides,” *Applied Surface Science*, vol. 587, Article ID 152884, 2022.
- [30] J. F. Ying, B. J. Flinn, M. Y. Zhou, P. C. Wong, K. A. R. Mitchell, and T. Fostert, “Optimization of zinc phosphate coating on 7075-T6 aluminum alloy,” *Progress in Surface Science*, vol. 50, no. 1–4, pp. 259–267, 1995.
- [31] S. E. Hernández Martínez, “Structure and properties of AA 7075 reinforced with nanometric ZrO₂ obtained by ball-milling,” *Acta Metallurgica Sinica*, vol. 4, pp. 2703–2709, 2014.
- [32] V. Sivamaran, D. V. Balasubramanian, D. M. Gopalakrishnan, D. V. Viswabaskaran, D. A. G. Rao, and D. G. Sivakumar, “Mechanical and tribological properties of Self-Lubricating Al 6061 hybrid nano metal matrix composites reinforced by nSiC and MWCNTs,” *Surfaces and Interfaces*, vol. 21, Article ID 100781, 2020.
- [33] V. Sivamaran, V. Kavimani, M. Bakkiyaraj, and S. T. Selvamani, “Multi response optimization on tribo-mechanical properties of CNTs/nSiC reinforced hybrid Al MMC through RSM approach,” *Forces in Mechanics*, vol. 6, Article ID 100069, 2022.
- [34] R. Karunanithi, K. S. Ghosh, and S. Bera, “Synthesis and characterization of TiO₂ dispersed Al 7075 micro- and nanocomposite,” *Advanced Materials Research*, vol. 984-985, pp. 313–318, 2014.
- [35] N. Barati, E. I. Meletis, F. Golestani Fard, A. Yerokhin, S. Rastegari, and M. A. Faghihi-Sani, “Al₂O₃-ZrO₂ nanostructured coatings using DC plasma electrolytic oxidation to improve tribological properties of Al substrates,” *Applied Surface Science*, vol. 356, pp. 927–934, 2015.
- [36] S. E. Hernández-Martínez, J. J. Cruz-Rivera, C. G. Garay-Reyes, C. G. Elias-Alfaro, R. Martínez-Sánchez, and J. L. Hernández-Rivera, “Application of ball milling in the synthesis of AA 7075-ZrO₂ metal matrix nanocomposite,” *Powder Technology*, vol. 284, pp. 40–46, 2015.
- [37] V. Sivamaran, V. Balasubramanian, M. Gopalakrishnan, V. Viswabaskaran, and A. G. Rao, “Identification of appropriate catalyst system for the growth of multi-walled carbon nanotubes via catalytic chemical vapor deposition process in a single step batch technique,” *Materials Research Express*, vol. 6, no. 10, Article ID 105620, 2019.
- [38] J. F. Ying, M. Y. Zhou, B. J. Flinn, P. C. Wong, K. A. R. Mitchell, and T. Foster, “The effect of Ti-colloid surface conditioning on the phosphating of 7075-T6 aluminium alloy,” *Journal of Materials Science*, vol. 31, no. 3, pp. 565–571, 1996.
- [39] S. Shenbag, N. Moorthi, and V. Moorthi, “Aluminium-titanium diboride (Al-TiB₂) metal matrix composites: challenges and opportunities,” *Procedia Engineering*, vol. 38, pp. 89–97, 2012.
- [40] M. Anil, V. C. Srivastava, M. K. Ghosh, and S. N. Ojha, “Influence of tin content on tribological characteristics of spray formed Al-Si alloys,” *Wear*, vol. 268, no. 11-12, pp. 1250–1256, 2010.
- [41] F. Muhaffel, M. Baydogan, and H. Cimenoglu, “A study to enhance the mechanical durability of the MAO coating fabricated on the 7075 Al alloy for wear-related high

- temperature applications,” *Surface and Coatings Technology*, vol. 409, Article ID 126843, 2021.
- [42] S. E. Hernández-Martínez, J. J. Cruz-Rivera, C. G. Garay-Reyes, R. Martínez-Sánchez, I. Estrada-Guel, and J. L. Hernández-Rivera, “Comparative study of synthesis of AA 7075-ZrO₂ metal matrix composite by different mills,” *Journal of Alloys and Compounds*, vol. 643, no. S1, pp. S107–S113, 2015.
- [43] E. Tolun and S. Tolun, “On the comparison of the ballistic response of coated aluminum plates,” *Materials & Design*, vol. 31, no. 7, pp. 3188–3193, 2010.